

Fast extended-x-ray-absorption-fine-structure spectroscopy with a laser-produced x-ray pulse

P. J. Mallozzi, R. E. Schwerzel, H. M. Epstein, and B. E. Campbell

Battelle, Columbus Laboratories, 505 King Avenue, Columbus, Ohio 43201

(Received 11 August 1980)

Extended-x-ray-absorption-fine-structure (EXAFS) spectra of aluminum and magnesium have been measured with single nanosecond pulses of soft x rays generated by laser-produced plasmas. This technique provides a practical alternative to synchrotron radiation for the acquisition of EXAFS data for elements having atomic numbers up to 40. It also provides a unique capability for the analysis of molecular structure in highly transient chemical species.

I. INTRODUCTION

The extended x-ray-absorption-fine-structure (EXAFS) technique is a powerful new tool for studying molecular structure. EXAFS provides information on the identities and spatial arrangement of the atoms in any type of solid, liquid, or gas, even those composed of highly complex molecules. In the EXAFS technique, the x-ray absorption coefficient of a material is measured as a function of energy from the *K* edge or *L* edge of a specific element in the material to as far as 1000 eV above the edge.^{1,2} The absorption of x rays by the element is accompanied by the ejection of photoelectrons, which can be scattered from neighboring atoms. Backscattering of these photoelectrons from atoms in the immediate vicinity of the absorbing atom gives rise to a periodic "wiggle" structure in the x-ray absorption spectrum.^{1,3,4} By analyzing this wiggle structure above the absorption edge of a particular element, information can be obtained about the spatial arrangement of atoms in the immediate vicinity of the absorbing species. Since only the nearby atoms are involved, long-range order is not required; therefore, the EXAFS technique can be applied to the study of a broad class of materials, including liquids, gases, and amorphous or crystalline solids.

Conceptually, the EXAFS phenomenon may be described in the following manner. The wave function of the photoelectron (the final state of the x-ray-absorption transition) consists of an outgoing part and a scattered part, which overlap near the origin, where the wave function of the initial (bound) state of the electron is concentrated. The overlap produces an interference which is either constructive or destructive, depending on the wave number

$$k = 2\pi/\lambda = 1/\hbar [2m(E - E_{\text{edge}})]^{1/2}$$

of the photoelectron. When the interference is constructive, the increased amplitude near the

origin results in an enhanced absorption coefficient. When the interference is destructive, the absorption coefficient is diminished. Thus, the relative phase relationship between the outgoing and incoming photoelectrons is changed by varying the photon energy of the incident x-rays, causing a periodic modulation in the absorption coefficient. The modulation can be interpreted on the basis that each atom (or shell of atoms) surrounding the absorbing atom will contribute a single modulated sine wave in *k* to the absorption coefficient.

In the past, chemical-structure research with the EXAFS technique has been limited by the lack of suitably intense sources of x rays. This deficiency is now being remedied to some extent by the increasing availability of synchrotron radiation, which is being harnessed in a number of x-ray test facilities throughout the world.⁵ There are certain types of EXAFS experiments, however, which cannot be performed easily with synchrotron x-ray sources. Most significant, perhaps, are those experiments which are designed to analyze highly transient structures such as chemically reactive intermediates or the excited electronic states of molecules. These experiments could be carried out if it were possible to obtain a complete EXAFS spectrum with a single, intense, short pulse of x rays synchronized with the optical or electrical excitation of the sample.

Previous work in our laboratories has indicated that laser-produced plasmas should be nearly ideal x ray sources for fast kinetic studies of this type.⁶ Indeed, we have recently reported the first experimental demonstration of the feasibility of performing EXAFS measurements with laser-produced x rays.⁷ These experiments show that it is possible to obtain well-resolved EXAFS spectra of light elements (atomic numbers ranging up to about 40) with a single nanosecond pulse of soft x rays produced with a neodymium-doped-glass laser. In the present paper we discuss in detail the techniques and results of our experiments to date.

II. GENERAL TECHNIQUE AND MAIN RESULT

The basic experimental configuration used in the experiments is shown in Fig. 1. In a typical experiment, an infrared laser pulse with an energy of approximately 100 J and a pulse width of approximately 3.5 ns (full width at half maximum) is focused onto a solid metal slab target, thereby creating a surface plasma and raising it to the kilovolt temperature regime by means of the inverse bremsstrahlung absorption process. The laser pulse strikes a 100- to 200- μm diameter focal spot at an incident intensity of about 10^{14} W/cm². The resulting x-ray spectrum is dispersed by Bragg reflection from a flat crystal and recorded on photographic film. The position and range of the recorded spectrum can be varied easily by adjusting the size and position of the dispersing crystal as desired. As Fig. 1 indicates, the system is so arranged that the thin-film sample occupies one-half of the x-ray beam. The reflected (diffracted) x rays thus form a double image on the photographic film, with the reference portion of the reflected beam striking the top half of the film and the sample portion of the beam striking the lower half of the film. In this way, the entire spectrum is recorded at once using a single laser pulse. The absorption (EXAFS) spec-

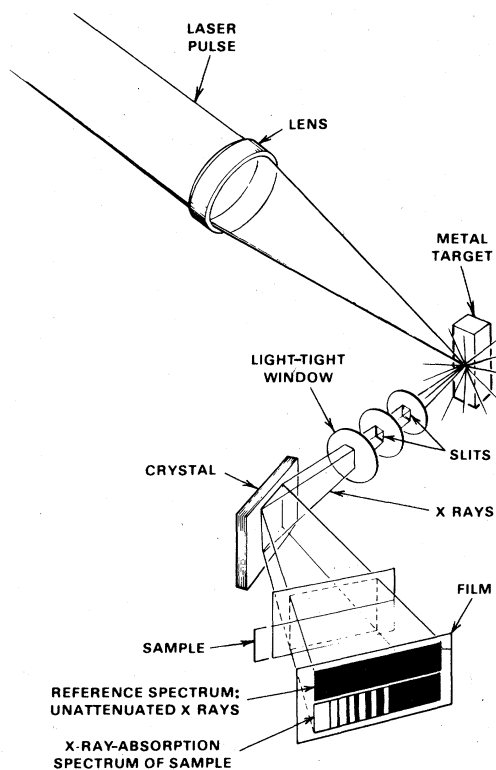


FIG. 1. Schematic view of laser-EXAFS experimental configuration.

trum can easily be extracted from the data since both the incident and transmitted x-ray intensities are known for each wavelength.

We have chosen to use film because the need to record the entire spectrum in a few nanoseconds rules out detectors based on the counting of individual photons. Film is the simplest alternative and, when evaluated by digital densitometer techniques, is capable of high resolution and contrast discrimination. With proper choice of film type, grain size, exposure, and data handling, it is possible to obtain results approaching the statistical limit allowed by the incident x-ray photon fluence. Because the photographic film is a non-linear recording medium, it is necessary to multiply the measured optical densities by a known response factor to determine the absolute x-ray flux at each wavelength. This numerical data handling is done with an online minicomputer.

The capabilities of this technique are illustrated by the *K*-edge laser-EXAFS spectra shown in Figs. 2 and 3, taken with aluminum and magnesium samples.⁸ These spectra are representative of our results to date, and each was obtained with the x rays produced by a single laser pulse incident on a metal slab target. The target used for the aluminum EXAFS spectrum was iron, whereas the target used for the magnesium spectrum was chromium. These target materials produce mainly continuum emission in the vicinity of the *K* edges they were used to study. Line radiation increases the probable error in data reduction, and should be avoided as much as possible. A KAP (potassium acid phthalate) crystal was used to obtain the aluminum spectrum, and a RAP (rubidium acid phthalate) crystal was used for the magnesium spectrum.

III. EXPERIMENTAL APPARATUS AND METHOD

In this section, questions relating to targets, crystals, samples, and other features of the tech-

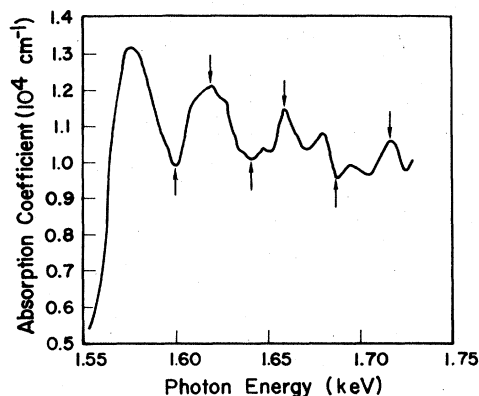


FIG. 2. Laser-EXAFS spectrum of aluminum foil.

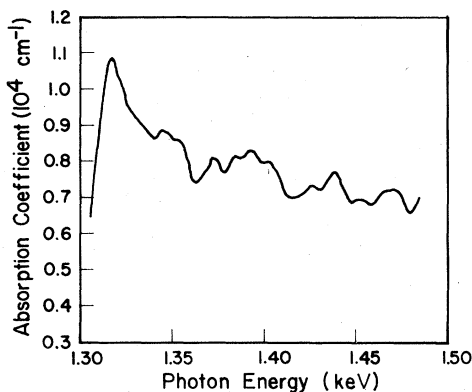


FIG. 3. Laser-EXAFS spectrum of magnesium film.

nique will be discussed in more detail. For clarity, specific data will be given only for the aluminum measurements. The discussion will converge on an evaluation of the potential sensitivity of the technique under the actual operating conditions of the experiment.

Aside from the laser and beam-focusing apparatus, which have already been discussed, the basic experimental apparatus consists of a modified General Electric XRD-7 vacuum x-ray spectrometer with the x-ray tube replaced by the laser-plasma x-ray source. The laser target is mounted on a remotely controlled XYZ translation stage to permit a change of targets or target position in the vacuum. The crystal angle is also remotely controlled and can be adjusted in the vacuum.

The iron target used to produce the aluminum EXAFS spectrum emits both continuum and line radiation. The lines above $h\nu \approx 1$ keV are bunched into an *L* group, which lies mostly below 1.5 keV, and a *K* group, which lies above about 5 keV. The region between 1.5 and 5 keV is mostly continuum radiation with a characteristic plasma bremsstrahlung temperature of approximately 800 eV. For the purpose of planning experiments, using the experimental parameters and configuration described earlier, the following formula for this continuum radiation has proved useful:

$$I(h\nu) = \frac{0.025}{2\pi R^2} \exp\left(\frac{-h\nu}{800}\right), \quad (1)$$

expressed in units of $J/eV\text{ cm}^2$, where R is the distance from the x-ray source (laser target) to an observer, and $h\nu$ is the photon energy in eV. It should be noted that the *K* edge of aluminum ($E_K = 1560$ eV) lies in the most intense portion of the iron continuum, just above the iron *L* group. This method of matching target with sample seems reasonable when studying x-ray edges in the 1–2-keV regime, e.g., when studying *K* edges of ele-

ments with atomic numbers $Z \approx 10$ –20 and *L* edges of elements with atomic numbers $Z \approx 20$ –40. It appears that the appropriate targets for such studies have atomic numbers in the range $Z \approx 20$ –30.

The KAP crystal used to disperse the x rays in the aluminum EXAFS experiments was 1 cm wide and 2.5 cm long, and was located approximately 10 cm from the x-ray source. The x rays are reflected from the crystal according to the formula $2d \sin\theta = m\lambda$, where θ is the Bragg angle, i.e., the angle of incidence measured with respect to the crystal plane. Since the $2d$ spacing of KAP is 26.64 \AA , $\theta \approx 17^\circ$ for first-order reflection ($m = 1$) of x rays at the *K* edge of the aluminum sample. The rocking-curve width (i.e., the full width at half maximum of the intensity versus angle profile for monochromatic x rays) of the crystal at this angle is 1.2×10^{-4} rad, corresponding to an energy spread $\Delta h\nu \approx 0.6$ eV. The reflection efficiency at the peak of the rocking curve at this angle is about 5%.

The data given above may be used to calculate the number of photons per eV that strike the film. This quantity can then be used to evaluate the sensitivity with which the x-ray absorption coefficient can be measured. A convenient starting point for the calculation is Eq. (1). This formula tells us that the x-ray fluence at the KAP crystal, which is located at a distance $R = 10$ cm from the x-ray source, in the energy region just above the *K* edge (i.e., just above $h\nu \approx 1560$ eV), is

$$\begin{aligned} 0.025 \times 1/(2\pi 10^2) \exp(-1560/800) \\ \text{or} \\ (5.7 \times 10^{-6})(6 \times 10^{18})/1560 \\ = 2.2 \times 10^{10} \text{ photons/eV cm}^2. \end{aligned}$$

To obtain the number of photons per eV that are reflected from the crystal, we multiply this number by the area of a narrow rectangle whose length is equal to the width of the crystal (1 cm) and whose width is R times the rocking-curve width (1.2×10^{-4} rad), and also multiply it by the reflection efficiency (0.05) of the crystal. We thus arrive at the result

$$(2.2 \times 10^{10}) [(1)(10)(1.2 \times 10^{-4})] 0.05 = 1.3 \times 10^6$$

photons/eV for the number of photons reflected from the crystal.

The figure 1.3×10^6 ignores attenuation through the sample, which is approximately 2 x-ray mean free paths thick. What really matters in determining the sensitivity of the absorption-coefficient measurement is the number of photons that strike

the film after passage through the sample. This number is readily calculated to be $(1.3 \times 10^6)1/e^2 = 2 \times 10^5$ photons/eV.

In analyzing the data, the energy spectrum was divided into 5-eV energy intervals. There are therefore approximately $5(2 \times 10^5) = 10^6$ photons in each energy interval. In principle, this allows an interval-to-interval contrast of $\Delta N/N = 1/N^{1/2} \approx 10^{-3}$, or approximately 0.1%.

It should be remarked that the reason for using a sample thickness of two mean free paths is that this optimizes the contrast obtainable with a given sized energy interval. It should also be noted, for future reference, that two mean free paths optimize the resolution obtainable at a given contrast level.

The photographic film used to record the EXAFS spectra shown in Figs. 2 and 3 is Kodak NS-2T. This film was chosen because, under the particular conditions of these experiments, the data are produced in the "linear" range of the film, where the optical density is proportional to the log of the exposure. In order to minimize the effect of film nonlinearity, the "reference" portion of the x-ray beam reflected from the crystal is passed through a thin layer of Mylar whose thickness is adjusted to produce the same average exposure as the "sample" portion of the beam. Analysis of the film record was performed automatically with a video digitizer, which serves as a computerized densitometer. The wavelength calibration of the film record is accomplished by noting where well known x-ray lines generated by focusing the laser beam onto selected targets lie, and interpolating between them.

IV. ANALYSIS OF RESULTS

A convenient starting point for interpreting EXAFS spectra is the generally accepted formula¹

$$\chi(k) = \frac{m}{4\pi k^2} \sum_j \frac{N_j}{R_j^2} t_j(2k) \exp\left(\frac{-2R_j}{l}\right) \times \sin[2kR_j + 2\delta_j(k)] \exp(-2k^2\sigma_j^2). \quad (2)$$

Here $\chi(k)$ is the fractional modulation of the absorption coefficient due to EXAFS: $\chi(k) = (\mu - \mu_0)/\mu_0$, where μ_0 is the absorption coefficient for a single atom in a vacuum. The quantity

$$k = [0.262467(E - E_{\text{edge}})]^{1/2}$$

is the photoelectron wave vector in reciprocal angstroms, where E is energy in electron volts, m is the electron mass, \hbar is Planck's constant, N_j is the number of atoms scattering at the distance R_j , $t_j(2k)$ is the electron scattering matrix in the backward direction for atoms at R_j , l is the

mean free path of the electron, $\exp(-2\sigma_j^2 k^2)$ is a Debye-Waller factor due to thermal vibrations or static disorder with root-mean-square fluctuations σ_j , and $\sin[2kR_j + 2\delta_j(k)]$ is the sinusoidal interference term, $\delta_j(k)$ being the phase shift.

A full analysis of EXAFS spectra on the basis of Eq. (2) requires the use of computer-assisted Fourier-transform techniques.^{1,2} However, it is more illustrative for the present purpose to employ a straightforward graphical technique¹ to deduce the nearest-neighbor distance. This will be done for the aluminium edge shown in Fig. 2.

The graphical technique which we employ is based on Eq. (2) and stems from the fact that the EXAFS curve is usually dominated by scattering from the nearest neighbors. This is especially true of the positions of the principal maxima and minima, which are determined mainly by the first sine term in Eq. (2), namely, $\sin[2kR_1 + 2\delta_1(k)]$. If δ_1 is linear in k , then $\delta_1 = \alpha_1 k + \beta_1$, and the argument of the sine term takes the form $2k(R_1 - \alpha_1) + 2\beta_1$. The approximate positions of the maxima and the minima of the EXAFS curve are thus given by

$$n\pi = 2k(R_1 - \alpha_1) + 2\beta_1, \quad (3)$$

where $n = 0, 2, 4, \dots$ for maxima and $1, 3, 5, \dots$ for minima. A plot of n against k for the dominant maxima and minima of the EXAFS spectrum as shown in Fig. 2 is given in Fig. 4, with $k=0$ taken to correspond to the inflection point, $E_{k \text{ edge}} = 1552$ eV, of the measured x-ray absorption coefficient. The points closely fit a straight line with a slope $(2/\pi)(R_1 - \alpha_1)$ of 1.7 \AA . This leads to the basic result $(R_1 - \alpha_1) \approx 2.6 \text{ \AA}$. Since $R_1 \gg \alpha_1$ (α_1 is typically a few tenths of an angstrom), this result is in good agreement with the known nearest-neighbor distance of 2.86 \AA for the aluminum fcc lattice.⁹

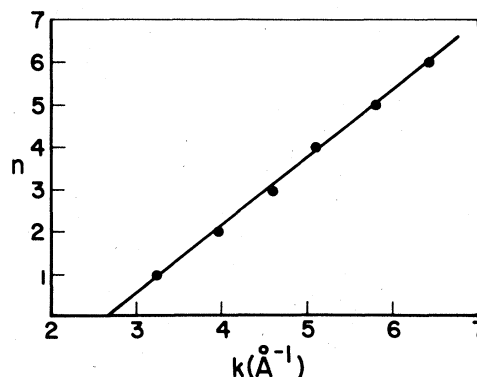


FIG. 4. Graph of n vs k for aluminum. The points correspond to the features indicated by arrows in Fig. 2.

The spectra presented in Figs. 2 and 3 are noteworthy for several reasons. They illustrate the capability of the laser-EXAFS technique to record EXAFS spectra of light elements with absorption edges below about 3 keV, which are difficult to study with other x-ray sources. The technique is particularly suitable at present for the study of *K*-edge EXAFS spectra of the elements from carbon to sulfur and of *L*-edge EXAFS spectra of the elements from sulfur to molybdenum. More important, however, the complete laser-EXAFS spectra presented in Figs. 2 and 3 were each obtained in only a few nanoseconds with a single pulse of laser-produced x rays. This represents a dramatic improvement in the speed and ease of obtaining EXAFS data compared to what is possible with other known x-ray sources. The technique also makes possible the measurement of

"flash-EXAFS" spectra of transient species having lifetimes of a few nanoseconds or less. Thus, with this technique it may soon be possible to make "snapshots" or "movies" of the structural changes that occur in molecules when they are excited by optical or other means. This capability is provided almost automatically by the pulsed nature of the laser-EXAFS measurement. Experiments along these lines are presently underway in our laboratory, and will be reported shortly.

ACKNOWLEDGMENTS

This work was supported by the U. S. Air Force Office of Scientific Research and Battelle Memorial Institute, Corporate Technical Development.

¹D. E. Sayers, F. W. Lytle, E. A. Stern, *Adv. X-Ray Anal.* **13**, 248 (1970); F. W. Lytle, D. E. Sayers, E. A. Stern, *Phys. Rev. B* **11**, 4825 (1975); E. A. Stern, D. E. Sayer, F. W. Lytle, *ibid.* **11**, 4836 (1975).

²P. Eisenberger and B. M. Kincaid, *Science* **200**, 1441 (1978); S. P. Cramer, T. K. Eccles, F. Kutzler, K. O. Hodgson, S. Doniach, *J. Am. Chem. Soc.* **95**, 8059 (1976); S. P. Cramer and K. O. Hodgson, *Prog. Inorg. Chem.* **25**, 1 (1979).

³R. de L. Kronig, *Z. Phys.* **70**, 317 (1931); **75**, 191 (1932); **75**, 468 (1932); H. Peterson, *ibid.* **98**, 569 (1936).

⁴C. A. Ashley and S. Doniach, *Phys. Rev. B* **11**, 1279 (1975); P. A. Lee and J. B. Pendry, *ibid.*, **11**, 2795 (1975).

⁵A. L. Robinson, *Science* **190**, 1074 (1975); W. D. Metz and A. L. Robinson, *ibid.* **190**, 1186 (1975); H. Winick and A. Brennstock, *Annu. Rev. Nucl. Part. Sci.*

28, 33 (1978).

⁶P. J. Mallozzi, H. M. Epstein, R. G. Jung, D. C. Applebaum, B. P. Fairand, and W. J. Gallagher, in *Fundamental and Applied Laser Physics: Esfahan Symposium*, edited by M. S. Feld, A. Javan, and N. A. Kurnit, (Wiley-Interscience, New York, 1973), pp. 165-220; P. J. Mallozzi, H. M. Epstein, R. E. Schwerzel, *Adv. X-Ray Anal.* **22**, 267 (1978).

⁷P. J. Mallozzi, R. E. Schwerzel, H. M. Epstein, and B. E. Campbell, *Science* **206**, 353 (1979).

⁸The aluminum foil was free standing, and was purchased from Reactor Experiments, Inc. The magnesium foil was vapor deposited onto a 2 μm thick Mylar substrate, and contained an undetermined amount of oxide impurities.

⁹L. Pauling, *The Nature of the Chemical Bond*, 3rd ed. (Cornell University Press, Ithaca, New York, 1960), Chap. 11.